Coherent adiabatic theory of two-electron quantum dot molecules in external spin baths

R. Nepstad,[1] L. Sælen,[1,2] and J. P. Hansen[1]

[1]*Department of Physics and Technology, University of Bergen, N-5007 Bergen, Norway*
[2]*Laboratoire de Chimie Physique-Matiére et Rayonnement, Université Pierre et Marie Curie, 11, Rue Pierre et Marie Curie 75231 Paris Cedex 05, France*

We derive an accurate molecular orbital based expression for the coherent time evolution of a two-electron wave function in a quantum dot molecule where the electrons interact with each other, with external time dependent electromagnetic fields and with a surrounding nuclear spin reservoir. The theory allows for direct numerical modeling of the decoherence in quantum dots due to hyperfine interactions. Calculations result in good agreement with recent singlet-triplet dephasing experiments by Laird *et. al.*[Phys. Rev. Lett. **97**, 056801 (2006)], as well as analytical model calculations. Furthermore, it is shown that using a much faster electric switch than applied in these experiments will transfer the initial state to excited states where the hyperfine singlet-triplet mixing is negligible.

PACS numbers: 73.21.La, 78.67.-n, 85.35.Be, 78.20.Bh

It is now well recognized that the hyperfine interaction is one of the main sources of decoherence in few-electron quantum dots. This interaction, originally considered in metals by Overhauser more than 50 years ago [1], couples the electronic spin states through weak nuclear spin interactions with an order of $\sim 10^6$ surrounding nuclei [2]. Recently, this coupling has received considerable interest through the demonstration of controlled single electron manipulation [3, 4] which opens for real quantum information processing based on electronic spin states in quantum dots [5]. Procedures to minimize or control the hyperfine interaction is therefore vital for the functioning of any quantum dot based information processing technology. Such mechanisms also contain novel aspects of spin de- and re-phasing of quantum systems interacting with a large spin bath.

Recently it was demonstrated in experiments [6, 7] with two-electron quantum dot molecules that the magnitude of the hyperfine interaction is consistent with a random magnetic field strength of a few mT. The nuclear field-induced singlet-triplet coupling leads to a spin dephasing of an initially prepared singlet state within $1-10$ ns. These experiments utilize fast adiabatic electric switching techniques which transform the ground state from a two-electron ionic state in one dot to a covalent state with one electron in each dot.

The experiments have been analyzed in detail theoretically based on various model Hamiltonians [8, 9]: For small tunneling coupling the effective two-electron Hilbert space amounts to the four possible covalent spin states (a singlet and three triplet states). This may be further reduced to two states by exposing the molecule to a magnetic field which decouple the two states with nonzero magnetic quantum numbers. Within this approximation it was shown that the hyperfine interaction induce a spin saturation which saturates sensitively as a function of the exchange coupling and the hyperfine coupling [9]. These predictions were confirmed experimentally by Laird *et. al.* [10].

In the present Letter we develop a full coherent model of the two-electron spin dynamics which includes the hyperfine interaction on equal footing with the time dependent external fields. The results may be directly compared with the experimental results. The theory not only validates the effective two-level models in the presence of an external magnetic field, but also demonstrates predictive saturation values in the absence of an external magnetic field. Furthermore, it will be shown that decreasing the switching time an order of magnitude may lead to controlled diabatic transfer [11] to excited states where the singlet-triplet mixing can be neglected.

Our starting point is the Hamiltonian of two interacting electrons in a double quantum dot with dot separation d as recently applied in studies of electron structure as well as in studies of photon induced controlled transport. [12, 13, 14],

$$\widehat{\mathrm{H}} = h(\mathbf{r}_1) + h(\mathbf{r}_2) + \frac{e^2}{4\pi\epsilon_r\epsilon_0 r_{12}} \tag{1}$$

where

$$\begin{aligned}\hat{h}\,(x,y) \;=\; & -\frac{\hbar^2}{2m^*}\nabla^2 + \frac{1}{2}m^*\omega^2\left[\left(|x| - \frac{d}{2}\right)^2 + y^2\right] \\ & + \frac{e^2}{8m^*}B_{ext}^2(x^2+y^2) + \frac{e}{2m^*}B_{ext}L_z \\ & + \gamma_e B_{ext}S_z + e\xi(t)x.\end{aligned} \tag{2}$$

Here $\mathbf{r}_{1,2}$ are single-particle coordinates, ξ is an electric time dependent field applied along the inter-dot axis and B_{ext} is an external magnetic field perpendicular to the dot. The material parameters are taken as those of GaAs, with effective mass $m^* = 0.067m_e$ and relative permittivity $\epsilon_r = 12.4$. The gyromagnetic ratio for GaAs is $\gamma_e = g^*\frac{e}{2m_e}$, with $g^* = -0.44$. The confinement strength is set to $\hbar\omega = 1$ meV and the inter-dot separation to $d = 130$ nm, which are realistic experimental values [4, 15].

Fig. 1 shows the energy spectrum obtained from diagonalization with $B_{ext} = 0$ and $B_{ext} = 200$ mT (inset). The spectrum of the system has been explained in detail elsewhere [13]. For $B_{ext} = 0$ symmetry about the y-axis is conserved and we show only the singlet and triplet ($m_s = 0$) eigenstates corresponding to the three lowest energy bands with even reflection symmetry. This symmetry is broken when the external magnetic field is applied and all states are shown.

When $B_{ext} \neq 0$ the magnetic sub-levels split (not shown). In addition to the splitting of the spin states (anomalous Zeeman effect) the spectrum is also changed by the Zeeman (L_z) and diamagnetic (B_{ext}^2) terms, as seen clearly in the inset. The most important effects of these terms are the modified singlet-triplet splitting J, the modified anti-crossing energy difference and the splitting of the second band according to the sign of the angular momentum expectation value, $\langle L_z \rangle$.

It is particularly worth noting that the energy spectrum exhibit several near degenerate anti-crossing regions where the coupling strength can be tuned in experiments through adjustable gate voltages and switching times [10]. Restricted by conservation of total spin, the states can couple dynamically as the electric field varies. The relative coupling strength from our model is shown in the lower panel of Fig. 1. The strongest coupling strength is seen between the singlet ground state and first excited states at -0.013 mV/nm. This puts a limit on the switching time through the region enclosed by a green circle for adiabatic time development along the initial singlet ground state, marked as 'I' in Fig. 1. On the other hand, a very rapid transfer can lead to diabatic development, to be discussed later.

The few and well defined states resulting from the present diagonalization suggest that the time evolution is most precisely described in an adiabatic basis of instant eigenstates of the time-dependent Hamiltonian of Eq. (1), $\widehat{H}(t)\chi(\mathbf{r}_1, \mathbf{r}_2; \xi) = \epsilon(\xi)\chi(\mathbf{r}_1, \mathbf{r}_2; \xi)$, where the energies $\epsilon(\xi)$ depend parametrically on the time-dependent electric field. We expand the wavefunction in these basis states,

$$\Psi(\mathbf{r}_1, \mathbf{r}_2, t) = \sum_k c_k(t)\chi_k(\mathbf{r}_1, \mathbf{r}_2; \xi) \otimes |S\rangle \qquad (3)$$

where k runs over all basis states. Projecting onto each basis state, the following expression for the time evolution of the amplitudes is obtained,

$$\dot{c}_k(t) = \dot{\xi} \sum_{j \neq k} \frac{\langle \chi_k | X | \chi_j \rangle}{\epsilon_k - \epsilon_j} c_j(t) + \imath \epsilon_k(\xi) c_k(t), \qquad (4)$$

with $X = x_1 + x_2$.

Additional terms can readily be included as extra matrix elements in the expression above. To study hyperfine interactions, spin couplings for $\sim 10^6$ nuclear spins surrounding the electrons must be included. These evolve in time, but on a much longer time scale than we will consider here. We therefore use the quasistatic approximation [8, 16], neglecting their time dependence. In addition, the large number of spins justifies a semiclassical approximation [17], where all the nuclear spins are described by a single classical magnetic field. The hyperfine interaction is then given by

$$\widehat{H}_N = \gamma_e \sum_{i=1,2} \mathbf{S}_i \cdot \mathbf{B}_N(r_i), \qquad (5)$$

where S_i is the spin operator of electron i. Generally the direction of nuclear magnetic field $\boldsymbol{B}_N$ is random (no polarization) and the magnitude varies according to a normal distribution about zero, $P(\boldsymbol{B}_N) = 1/(2\pi B_{\rm nuc}^2)^{\frac{3}{2}} \exp\left(-\boldsymbol{B}_N \cdot \boldsymbol{B}_N / 2B_{\rm nuc}^2\right)$ [9]. $B_{\rm nuc}$ can be determined by experiments and is of the order of 1 mT [4]. The precise spatial variation of the nuclear magnetic field $\boldsymbol{B}_N$ is in general unknown, but also of less importance. The essential feature in the spin dephasing mechanism is the difference in effective magnetic fields between the two dots. The simplest way to represent this is by a step function,

$$\mathbf{B}_N = \begin{cases} (B_x\hat{\mathbf{e}}_x + B_y\hat{\mathbf{e}}_y + B_z\hat{\mathbf{e}}_z) & \text{, for } x \geq 0 \\ 0 & \text{, otherwise} \end{cases} \qquad (6)$$

This induces coupling between the singlet and triplet states

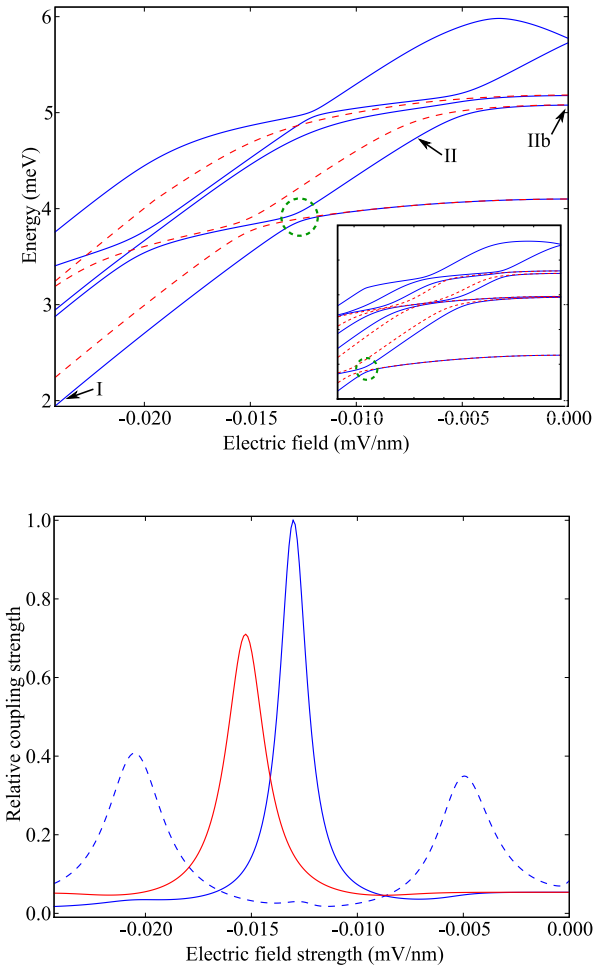

FIG. 1: (color online) Upper panel shows a few of the lowest energy levels as a function of electric field in the x-direction, corresponding to y-symmetric states. Inset shows the effect of an external magnetic field (200 mT) on the spectrum. Lower panel shows the relative coupling strengths of selected states; Full blue curve is $\langle 1, S|X|0, S\rangle$ between the two lowest singlet states (full blue curve), full red curve is $\langle 1, T_0|X|0, T_0\rangle$ between the two lowest triplet states and $\langle 3, S|X|1, S\rangle$ dashed blue curve is between the second lowest and third lowest singlet. Note that the $m_s = \pm 1$ triplet states are not shown.

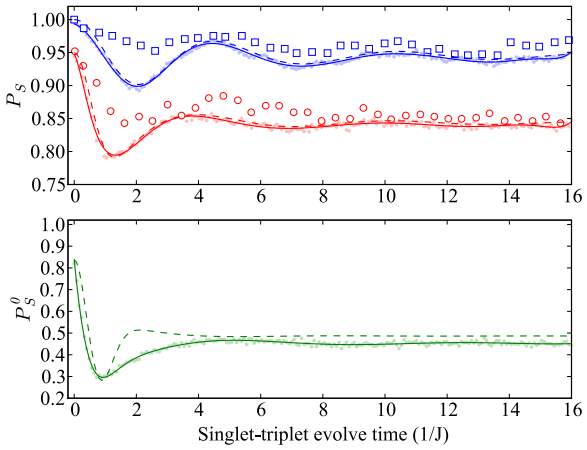

FIG. 2: (color online) Upper panel: Averaged time evolution of singlet component with $B_{ext} = 200$ mT. $B_N/J = 0.4$ (full blue line) and $B_N/J = 0.91$ (full red line, downshifted 5%). Squares and circles are experimental data taken from [10]. Prediction from two-level model shown as dashed lines. Semitransparent dots are actual numerical data, full lines are obtained from a smoothed spline interpolation. Lower panel: $B_N/J = 0.91$, but without external magnetic field. Prediction from four-level model (dashed line), scaled to match at $t = 0$.

and between the different triplet states.

From Eqs. (1,3,6) the time evolution of the wavefunction at zero electric field, restricted to the four lowest energy states $\{|S\rangle, |T_0\rangle, |T_-\rangle, |T_+\rangle\}$, becomes,

$$\dot{\mathbf{c}}(t) = \imath\gamma_e \begin{pmatrix} J/\gamma_e & B_z & \frac{B_x - \imath B_y}{\sqrt{2}} & -\frac{B_x + \imath B_y}{\sqrt{2}} \\ B_z & 0 & 0 & 0 \\ \frac{B_x + \imath B_y}{\sqrt{2}} & 0 & -B_{ext} & 0 \\ -\frac{B_x - \imath B_y}{\sqrt{2}} & 0 & 0 & B_{ext} \end{pmatrix} \mathbf{c}(t). \tag{7}$$

This expression is identical to four-level models previously considered [8]. We have here, however, excluded the inter-triplet couplings as this will allow us to obtain an analytical solution. When the external magnetic field is sufficiently strong, the $m_s = \pm 1$ triplet components effectively decouple, and we are left with a two-level system defined by the upper left part of the four-level matrix. Furthermore, since the triplet sub-levels are degenerate, the four-level matrix for $B_{\rm ext} = 0$ may be represented by an effective "radial" two-level model. In both cases we obtain the time evolution of the singlet coefficient

$$|c_S(t)|^2 = 1 - \frac{4B^2}{4B^2 + J^2} \sin^2\left(\frac{1}{2} t \sqrt{4B^2 + J^2}\right), \tag{8}$$

with $B = B_z$ for $B_{ext} \gg J$ and $B = \sqrt{B_x^2 + B_y^2 + B_z^2}$ for $B_{ext} = 0$.

In Fig. 2 we show our results together with experimental results of Laird et. al [10] using $B_{ext} = 200$ mT (upper panel). To calculate the singlet-triplet dephasing we start out in the singlet ground state at large electric field, -0.024 mV/nm. The field is then switched adiabatically to zero within 1 ns and kept at zero a variable period of time, t_s up to 16 $J/\hbar$ ns, before being switched back to its original value. The procedure is repeated a number of times, with a random nuclear magnetic field drawn from a Gaussian distribution. Finally, the average of the singlet correlator is computed, $P_S = 1/N \sum_i |c_S^i(t_s)|^2$. The full lines in the upper ($B_{\rm ext} = 200$ mT) and lower panel ($B_{\rm ext} = 0$) of Fig. 2 are produced from a sample size of $N = 1000$ different nuclear fields. For clarity, we have interpolated the numerical data using splines with a smoothing requirement. The actual numerical points are shown as semi-transparent dots. Also shown, as dashed lines, are predictions from the two-level theory. An excellent agreement between the theoretical results are noted which indicate that effects of the electrical switch, excited states and geometry of the potential are of less importance in this case. The present results are also compared with experimental data, shown as dots and circles in the upper panel. We also observe a very good agreement with the experimental results. Here we have varied $B_{\rm nuc}$ as opposed to J which may be varied in experiments by tuning the gate voltages. As verified by the two-level models the dephasing process mainly relies on their ratio. It should be noted that results in the upper panel have been scaled according to $P_S(t) = 1 - V(1 - P_S^0(t))$, where $V = 0.40$ is a visibility parameter determined in the experiments, $P_S(t)$ is the experimental averaged correlator while $P_S^0(t)$ is the theoretical averaged correlator [10].

Setting the external magnetic field to zero leads to increased dephasing, since the $m_s = \pm 1$ states are now coupled to the initial singlet state. This is indeed what we observe in our simulations, as shown in the lower panel of Fig. 2. The four-level (effective two-level) model yields the result shown as a dashed line, scaled to match the numerical data at $t_s = 0$. At large evolve times, these are in good agreement. Numerical solution of the full four-level matrix suggests that the slight discrepancy around $t_s = 2$ is due to the neglected inter-triplet couplings in Eq. (7). In contrast to the two-level case, we observe in the four level case a $\sim$10% dephasing occurring during the switch or more precisely between the two passages of the avoided crossing circled out in Fig. 1. This is a result of a much more involved dynamical interplay between the states and result in the present theory to a reduction of P_S^0 at $t_s = 0$.

A completely new feature can be studied by introducing an ultrafast switching function which leads to diabatic passage through the anti-crossing, highlighted by the green circle in Fig. 1. This will transfer the system to the first excited singlet state where at zero electric field the singlet-triplet splitting is approximately 100 times greater compared to the ground state. Important to note is that states in the second energy band are like the ground state covalent states [13] with one electron in each dot. This makes the states well suited for single-electron gate operations unlike the states in the third energy band which resemble ionic states. In Fig. 3 the evolution of the three lowest energy singlet states are displayed as the system is rapidly switched from positions marked I to II

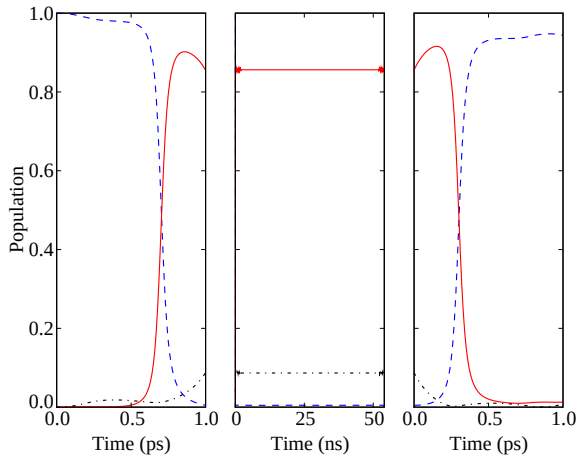

FIG. 3: (color online) The time evolution of the three most prominent states during the fast switch proceedure. About 95 % of the total norm is represented by these states, which are $|S,0\rangle$ (blue dashed), $|S,1\rangle$ (red full) and $|S,2\rangle$ (black dash-dotted). $B_{nuc} = 1$ mT ([1,1,1]). $B_{ext} = 0$. Left panel shows evolution during rapid switch (1 ps), center panel shows adiabatic passage to first excited state and evolution during dephasing period. Right panel shows rapid switching back to the one-well configuration (1 ps). Singlet-triplet coupling is weak for the excited singlet state, and thus only ~ 5 % is lost (mainly to other singlet states during switching).

in Fig. 1, using a nuclear magnetic field of 1 mT, and zero external magnetic field. From there it is transferred adiabatically from II to IIb. The leftmost panel shows the transfer of population from the ground to first excited state during a 1 ps switch, with around 10% of the population being further transported to the second excited state. In the middle panel, the system is switched adiabatically to zero electric field during 2 ns, and left to evolve here for 50 ns. The singlet-triplet coupling is completely suppressed, and when the system is switched back to position I, 95% of the initial singlet population is regained, the rest having vanished mostly to higher excited states during passage through the anti-crossings. The simulation was repeated a number of times with increasing nuclear magnetic field strength up to 10 mT, attributing only negligible changes to the dynamics. We note that by applying optimal control schemes the transition to excited states may be achieved with near 100% transition probability [11, 12, 18].

In conclusion, we have applied a first principle molecular orbital framework to accurately calculate the time development of the electronic states of a two-electron quantum dot molecule. For the first time the hyperfine interaction has been taken into account on the same coherent level as the time variation of the external electromagnetic fields. Calculations have displayed a very good agreement with experiments and a previously developed two-level model for experiments performed in static external magnetic fields. We have also performed full numerical calculations in absence of external magnetic field and predicted the dephasing dynamics by an effective four level model. Finally, we have pointed towards a new solution to the spin-dephasing problem by controlling and applying transitions between excited states.

This research has been supported by the Research Council of Norway (RCN). LS acknowledge financially support through a mobility grant from Université Pierre et Marie Curie.

[1] A. W. Overhauser, Phys. Rev. **92**, 411 (1953).
[2] A. V. Khaetskii, D. Loss, and L. Glazman, Phys. Rev. Lett. **88**, 186802 (2002).
[3] F. H. L. Koppens *et al.*, Nature **442**, 766 (2006).
[4] J. R. Petta, A. C. Johnson, C. M. Marcus, M. P. Hanson, and A. C. Gossard, Phys. Rev. Lett. **93**, 186802 (2004).
[5] D. Loss and D. P. DiVincenzo, Phys. Rev. A **57**, 120 (1998).
[6] F. H. L. Koppens *et al.*, Science **309**, 1346 (2005).
[7] J. R. Petta *et al.*, Science **309**, 2180 (2005).
[8] J. M. Taylor, J. R. Petta, A. C. Johnson, A. Yacoby, C. M. Marcus, and M. D. Lukin, Phys. Rev. B **76**, 035315 (2007).
[9] W. A. Coish and D. Loss, Phys. Rev. B **72**, 125337 (2005).
[10] E. A. Laird, J. R. Petta, A. C. Johnson, C. M. Marcus, A. Yacoby, M. P. Hanson, and A. C. Gossard, Phys. Rev. Lett. **97**, 056801 (2006).
[11] G. E. Murgida, D. A. Wisniacki, and P. I. Tamborenea, Phys. Rev. Lett. **99**, 036806 (2007).
[12] L. Saelen, R. Nepstad, I. Degano, and J. P. Hansen, Subm. to Phys. Rev. Lett. 2007.
[13] V. Popsueva, R. Nepstad, T. Birkeland, M. Førre, J. P. Hansen, E. Lindroth, and E. Walterson, Phys. Rev. B **76**, 035303 (2007).
[14] A. Harju, S. Siljamaki, and R. M. Nieminen, Phys. Rev. Lett. **88**, 226804 (2002).
[15] D. M. Zumbühl, C. M. Marcus, M. P. Hanson, and A. C. Gossard, Phys. Rev. Lett. **93**, 256801 (2004).
[16] I. A. Merkulov, A. L. Efros, and M. Rosen, Phys. Rev. B **65**, 205309 (2002).
[17] J. S. Briggs and J. M. Rost, Eur. Phys. Journ. D **10**, 311 (2000).
[18] E. Räsänen, A. Castro, J. Werschnik, A. Rubio, and E. K. U. Gross, Phys. Rev. Lett. **98**, 157404 (2007).